REPORT No. 552

WIND-TUNNEL TESTS OF 10-FOOT-DIAMETER AUTOGIRO ROTORS

By JOHN B. WHEATLEY and CARLTON BIOLETTI

SUMMARY

A series of 10-foot-diameter autogiro rotor models were tested in the N. A. C. A. 20-foot wind tunnel. Four of the models differed only in the airfoil sections of the blades, the sections used being the N. A. C. A. 0012, 0018, 4412, and 4418. Three additional models employing the N. A. C. A. 0012 section were tested, in which a varying portion of the blade near the hub was replaced by a streamline tube with a chord of about one-fourth the blade chord.

With maximum L/D used as a criterion, the order of merit of the airfoil sections tested is: N. A. C. A. 4412, 0012, 4418, and 0018. The elimination of blade area near the hub was found to have a detrimental effect on the rotor L/D. The results indicate the possibility of obtaining further improvements in the L/D by using thinner airfoil sections and by employing tapered blades with a tip chord smaller than the root chord. The results also demonstrate the necessity for a study of the effect of blade twist on the rotor characteristics and show the advisability of improving testing technique to reduce the errors occurring in the determination of the tare drag.

INTRODUCTION

The high-speed performance of the autogiro is at present inferior to that of the airplane, although no inherent reason for the existing large difference has appeared. The N. A. C. A. has accordingly decided to investigate different types of autogiro rotors with the purpose of establishing a means of improving the efficiency (the lift-drag ratio) of the rotor.

The results given in this paper were obtained by a wind-tunnel investigation of 10-foot-diameter model rotors in which the influence on rotor characteristics of the blade airfoil section and a variation in the blade plan form were determined. Four airfoil sections differing in camber and thickness and four plan forms were tested; the aerodynamic characteristics of each rotor were determined at several pitch settings over the entire range of tip-speed ratios in which the rotors would autorotate.

APPARATUS

The model rotors were tested in the N. A. C. A. 20-foot wind tunnel described in reference 1. The test set-up is shown in figure 1, which shows that the rotor was supported by a small mast projecting from a large fairing. The entire supporting structure, with the exception of the mast and part of the sting and tailpost also shown in figure 1, was shielded from the air stream to reduce the tare drag. The mast was attached to an electric motor enclosed in the shielding; the motor employed to start the model rotating was mounted in trunnion bearings to permit a change in the rotor angle of attack by means of the sting and tailpost. The rotors were mounted inverted so that at 90° angle of attack the rotor was upstream from the bulky supporting structure. A magneto tachometer geared to the rotor shaft measured the rotor speed.

The model rotor hub used for all rotor tests had journal bearings at the horizontal and vertical pin articulations; the use of these bearings made it necessary that the hub be considerably larger in proportion than a full-scale hub. The horizontal pin was placed at a radius of 1.125 inches (1.88 percent R) and the radius of the vertical pin was 2.50 inches (4.17 percent R). Damping was supplied at the vertical pins by means of adjustable washers, which provided a friction torque of about 6 inch-pounds. The rotor blades were attached to the hub by steel forks bolted to the blades and screwed into sockets connected to the vertical pins. Pitch adjustments were made at these screw connections, which were locked by clamping bolts. The blade butts were at 7½-inch radii (12.5 percent R) and the outer ends of the forks at 12-inch radii (20 percent R).

All seven rotors had diameters of 10 feet and consisted of three blades, which were constructed of laminated mahogany, hollowed to reduce their weight, balanced about the quarter-chord point by brass nosepieces forming part of the airfoil section. Four sets of blades differed only in the airfoil section used; the sections tested were the N. A. C. A. 0012, 0018,

4412, and 4418. These rotors are designated A (N. A. C. A. 0012), A (N. A. C. A. 4418), etc., where A indicates the plan form. Three additional sets of blades employing the N. A. C. A. 0012 profile were constructed in which a systematic variation of plan form was effected; these rotors are designated B (N. A. C. A. 0012), C (N. A. C. A. 0012), and D (N. A. C. A. 0012). Rotors B, C, and D differed in that the inner 30 percent, 45 percent, and 60 percent, respectively, of the blade was replaced by a 1¼-inch-diameter streamline tube having a chord of about one-fourth the blade chord, as shown in figure 2. The tip shape of all blades was semielliptical; the trailing edge was a circular quadrant with a radius of 0.75c, and the leading edge was an elliptical quadrant with axes of 0.25c and 0.75c. The physical characteristics of the blades are shown in table I; the ordinates of the airfoil sections are given in reference 2.

The motion of the rotor blade about the horizontal pin was recorded throughout several revolutions by a stylus scratching on waxed paper. The stylus was linked to the blade so that the deflections of the stylus and blade were proportional, and the waxed paper was wound on a drum concentric with the rotor axis immediately beneath the rotor disk. The record was oriented in azimuth by a prick punch fixed with reference to the air stream. Successive records were obtained by winding the paper on spools within the drum; the spools were manually operated from the balance house.

FIGURE 1.—A 10-foot autogiro rotor mounted for test.

TESTS AND PROCEDURE

Each rotor was tested at several pitch settings from 0° to the highest angle at which autorotation could be obtained over a reasonably wide range of tip-speed ratios. Pitch settings were measured from the angle of zero lift of the blade section using the data given in reference 2. The test data are incomplete in some cases at low tip-speed ratios and low pitch settings because at the lowest tunnel speed available (40 feet per second) the rotor speed became dangerously high. In general, the range of tip-speed ratios tested became smaller as the pitch setting was increased because autorotation broke down at successively lower values of the tip-speed ratio. No tests were made of the B (N. A. C. A. 0012) rotor at tip-speed ratios below 0.1 because the model vibrated violently in that range.

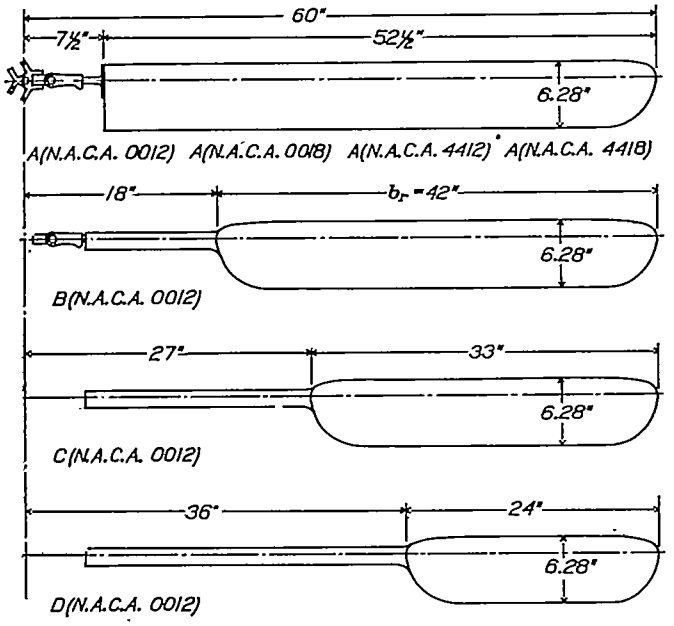

FIGURE 2.—Plan forms of model autogiro blades.

At the beginning of a test the rotor was driven at about 400 revolutions per minute with the electric motor. The tunnel fan was then started and the model was allowed to autorotate. In general, all tests were made at a rotor speed of 550 revolutions per minute, giving a tip speed of 288 feet per second. Data were obtained at each tunnel speed between 40 feet per second and 140 feet per second by adjusting the angle of attack. When the tunnel speed reached 140 feet per second, which corresponds to a tip-speed ratio of about 0.5 for a rotor speed of 550 revolutions per minute, it was kept constant and tip-speed ratios greater than 0.5 were obtained by successive reductions in the rotor speed. In this manner, except for the limitations previously mentioned, all tip-speed ratios from 0 to 0.7, corresponding to angles of attack from 90° to the minimum obtainable, were investigated.

At any tunnel speed, when steady conditions had been obtained, simultaneous visual observations of lift, drag, dynamic pressure, rotor speed, and angle of attack were made. Records of blade motion were obtained during the tests at intervals of the tip-speed ratio of about 0.03.

The tare forces on the set-up were determined with the rotor and hub removed over the same range of air speeds as that in which the rotor tests were made. There was an appreciable scale effect on the tare forces so that the coefficients of tare lift and drag used for correcting the observed data corresponded to the particular air speed at which the observed data were obtained. The method used for obtaining the tare forces results in the inclusion of the hub forces in the net lift and drag forces.

RESULTS

The terminology and symbols used in this paper are the same as those given in reference 3. For convenience, a list of the symbols and definitions follows:

V, true air speed, ft. per second.
Ω, angular velocity, radians per second.
R, rotor radius, ft.
α, rotor angle of attack, deg. (acute angle between relative wind and a plane perpendicular to the rotor axis).
L, rotor lift, lb.
D, rotor drag, lb.
T, rotor thrust, lb. (component of rotor force parallel to rotor axis).
θ, pitch setting, deg. (blade angle measured from zero lift position when blade is at rest).
C_L, lift coefficient, $\frac{L}{\frac{1}{2}\rho V^2\pi R^2}$
C_D, drag coefficient, $\frac{D}{\frac{1}{2}\rho V^2\pi R^2}$
C_R, resultant-force coefficient, $(C_L^2+C_D^2)^{\frac{1}{2}}$
C_T, thrust coefficient, $\frac{T}{\rho\Omega^2\pi R^4}$
μ, tip-speed ratio, $\frac{V\cos\alpha}{\Omega R}$
ψ, blade azimuth angle from down wind in direction of rotation, deg.
β, angle between blade axis and a plane perpendicular to rotor axis, deg. (positive in the direction of thrust), expressed by: $\beta=a_0-a_1\cos\psi-b_1\sin\psi-a_2\cos 2\psi-b_2\sin 2\psi-\ldots\ldots$
a_0, constant term in Fourier series that expresses β.
a_n, coefficient of $\cos n\psi$ in Fourier series that expresses β.
b_n, coefficient of $\sin n\psi$ in Fourier series that expresses β.
σ, solidity, ratio of blade area to swept disk area.
I_1, moment of inertia of one blade about the horizontal pin, slug-ft.^{2}
c, chord of blade, ft.
a, lift-curve slope with angle of attack, in radian measure.
γ, mass constant of blade, $\frac{c\rho aR^4}{I_1}$

The results of the force measurements corrected for tare and jet-boundary interference are presented in figures 3 to 40, inclusive. For each rotor, values of C_L, L/D, C_R, C_T, α, and the blade-motion coefficients a_0, a_1, and b_1 are presented in curve form for each pitch setting tested, as functions of the tip-speed ratio μ. The coefficients C_L, L/D, and C_R for the A (N. A. C. A. 4412) and A (N. A. C. A. 4418) rotors were cross-faired against the pitch setting and then replotted against tip-speed ratio, a procedure made possible in these cases by the large number of pitch settings tested. It will be noted that L/D has been given in preference to the drag coefficient C_D; this usage was found advisable because the minimum and maximum values of C_D were in the ratio of approximately 1:150 and an abnormal scale would have been required to present the results accurately.

The measured blade motion was transformed into the coefficients of a Fourier series by the 12-point harmonic analysis described in reference 4, resulting in a series of 12 terms. The blade motion of a full-scale rotor is such that the coefficients a_2 and b_2 are not negligible in comparison with a_0, a_1, and b_1. The mass constant γ of the model blades was so small, however, that all coefficients of order greater than the first were found to be equal to or smaller than the probable error in the results and, for this reason, no coefficients of higher order than the first have been included in the blade-motion data.

Figure 23 shows the effect of a variation in blade plan form on the maximum L/D for optimum pitch setting and on C_T at $\mu=0.35$. Figure 40 illustrates the effect of airfoil section on the maximum L/D and on C_T at $\mu=0.35$ as functions of the pitch setting. Figure 41 shows the significant effect of a change in the rotor speed on C_L and L/D; figure 42 shows the effect of rotor speed on a_1.

No test data on moments or centers of pressure were obtained; the geometry of the balance system rendered such results too inaccurate to be of value.

ACCURACY

The accidental errors occurring in these tests arise from nonsimultaneous observations, the human error in reading instruments, the failure to obtain steady conditions when taking data, and similar factors. The influence of these types of error on the final results has been minimized by obtaining a large number of test points during all tests.

There are three principal sources of consistent errors in the final results: The jet-boundary effect, the blocking effect in the tunnel, and the errors due to the method of obtaining the tare drag. A correction for the effect of the jet boundary on the rotor was applied by assuming the rotor to be equivalent to an airfoil of the same span and same total lift. This correction is justified principally by expediency, since no information exists that can be used for the accurate correction of the jet-boundary effect on a rotor. The use of this correction assumes a vortex field behind the rotor similar to the one behind the equivalent wing, an assumption obviously not exactly true. This error can, however, be considered small and especially so near maximum L/D, where the jet-boundary correction in all cases had almost vanished. The blocking effect, which is essentially a disturbance in the uniform velocity distribution across the jet by the presence of a body in the jet, has been estimated from disk tests to be as high as 20 percent for a disk normal to the air stream. Since this effect depends mostly upon the projected area of the body on a plane normal to the air stream, and upon the drag of the body, it can be neglected at angles of attack of less than 30° ($\mu>0.125$). Thus the blocking effect does not influence the maximum L/D, which occurs at $\mu=0.35$. The tare lift was small and the error arising from it can be neglected, but the tare drag is the source of an error of unknown magnitude. The tare forces were determined by testing the set-up with the rotor and hub removed, which leaves the interference effects in the net results; in addition, the hub drag, which was, because of the size of the hub, considerably greater than that of a full-scale rotor, was included in the net drag. These considerations indicate that the net drags obtained are appreciably larger than the correct values.

The nature of the consistent errors precludes an attempt at their evaluation; the following table summarizes the magnitude of the errors in the faired curves caused by the accidental factors:

μ	±3 percent.
α	±0.1°.
C_L	±3 percent.
L/D	±5 percent.
C_T	±3 percent.
a_0, a_1, b_1	±0.2°.

DISCUSSION

Before the detailed discussion, it is advisable to consider the effect of an erroneous tare drag on the results. As previously explained, the tare drag used was probably smaller than the correct value because the model rotor hub was disproportionately large. The net drag coefficients used in obtaining rotor lift-drag ratios are consequently considered too large. A constant decrement to the experimental net drag coefficients would increase the L/D at low-pitch settings more than at high-pitch settings because the rotor forces and coefficients increase with pitch setting. By reference to the curves of C_L and L/D it can be determined that C_L for maximum L/D at optimum pitch setting lies between 0.085 and 0.120 and occurs at $\mu=0.35$ for all rotors, showing that there is no great difference in the rotor forces at optimum pitch setting and, consequently, that the relative merit of

the different rotors will not be changed by a small error in the tare drag. The only important change will be a decrease in the optimum pitch setting and an increase in the values of the lift-drag ratios obtained.

Most of the results require little discussion. On all rotors an increase in angle of pitch setting increases the lift coefficient at any tip-speed ratio greater than that corresponding to maximum lift, which occurs at about $\mu=0.13$, and increases the thrust coefficient and the blade-motion coefficients at all tip-speed ratios. The lift-drag curves show that for each rotor there is an optimum angle of pitch setting considerably lower than the highest pitch setting at which autorotation occurs.

The variation of angle of attack with pitch setting is reasonably consistent. At tip-speed ratios in the approximate range 0 to 0.15 the angle of attack increases with pitch setting for pitch settings greater than 2°; at higher tip-speed ratios the angle of attack decreases with pitch setting until within 1° or 2° of the maximum pitch setting tested, at which point the angle of attack begins to increase.

A much greater range of operating pitch settings was obtained with the two cambered airfoils (N. A. C. A. 4412 and N. A. C. A. 4418) than with the two symmetrical ones (N. A. C. A. 0012 and N. A. C. A. 0018). The principal reason for this result is thought to be the twist of the blade during its operation. A twisting couple is applied to each blade if the normal component of the blade centrifugal force is not applied at the center of pressure of the air force. The centrifugal force is applied at the center of gravity of the blade, which is at 0.25c on all blades. The center of pressure of the symmetrical blades occurs also at 0.25c; consequently, the twisting moment on the symmetrical blades is negligible. The cambered blades, however, have a center of pressure that changes with angle of attack and has a mean position at about 0.35c. An upward force at 0.35c and an equal downward force at 0.25c obviously tend to decrease the blade pitch angle, which results in an operating pitch appreciably less than the pitch setting. This condition is illustrated in figure 40 by the difference in the thrust coefficients at equal pitch settings for the four airfoil sections used. The illustrated differences between the mean curve for the two symmetrical sections and the curves for the two cambered sections are then consistent with the explanation given when it is remembered that the N. A. C. A. 4418 is torsionally stiffer than the N. A. C. A. 4412 and that the N. A. C. A. 4418 and N. A. C. A. 4412 have almost identical center-of-pressure characteristics.

The preceding argument leads also to the conclusion that the twist, and consequently the rotor characteristics determined by the twist, will depend upon rotor speed because the centrifugal force and thrust vary with the square of the rotor speed, while the rigidity remains constant. This deduction is verified in figures 41 and 42, showing the A (N. A. C. A. 4412) rotor characteristics at 400 and 550 revolutions per minute. The lift coefficient L/D and the flapping coefficient a_1 at 7° pitch setting and 400 revolutions per minute correspond more closely to the characteristics for 8° than for 7° pitch setting when the test was made at 550 revolutions per minute. These curves show that at 400 revolutions per minute the operating pitch was greater than at 550 revolutions per minute although the pitch setting was the same.

The general information on maximum L/D is summarized in figures 23 and 40. Figure 40 shows that the order of merit of the airfoil sections based on maximum L/D is: N. A. C. A. 4412, 0012, 4418, and 0018, indicating that camber is advantageous and that a thickness of 18 percent is less efficient than one of 12 percent. Figure 23 shows that the maximum lift-drag ratio is affected adversely by reducing blade area near the hub. When quantitative conclusions are drawn from the results in this report, it is important to remember that the blade twist of the different airfoils was not constant; this factor may have influenced the relative L/D ratios of the rotors. It is therefore not known whether the increased efficiency of the cambered blades should be ascribed to the camber or the twist. The plan-form results also contain another variable, a change in solidity, which would affect the L/D; in this case, however, calculations indicate that the decrease in solidity should increase the L/D, whereas the sum of the two effects was a decrease in L/D. It then seems safe to conclude that the effect of reducing the blade area near the hub is, if anything, more disadvantageous than the results indicate.

The test results indicate that rotor efficiency can possibly be increased by extending the tests of blade thickness and by a further investigation of the effect of twist. The employment of tapered blades with the maximum chord at the hub also appears promising. The L/D results in this paper are, however, of only relative value because of the error inherent in the tare-drag results, and these values of L/D are at present exceeded on full-scale rotors with less efficient airfoil sections.

CONCLUSIONS

1. Cambered rotor blades with a center of gravity at 0.25c are appreciably reduced in pitch while operating because of the dynamic twist.

2. Owing to the different airfoil characteristics and possibly because of the blade twist, cambered blades develop a greater L/D than symmetrical ones.

3. An increase in blade thickness ratio from 12 percent to 18 percent results in an appreciably lower L/D.

4. The order of merit based on maximum L/D of the airfoil sections tested is: N. A. C. A. 4412, 0012, 4418, 0018.

5. Test results are quantitatively reliable for $\mu > 0.15$ except for the L/D, which is probably lower than the correct value.

6. Rotor lift-drag ratios are adversely affected by removing blade area near the hub.

7. A possibility exists of improving the rotor lift-drag ratio by tapering the blade to a smaller chord at the tip than at the hub.

8. The tests should be extended to include other airfoil sections and tapered blades, and the effect of blade twist should be carefully studied.

LANGLEY MEMORIAL AERONAUTICAL LABORATORY,
NATIONAL ADVISORY COMMITTEE FOR AERONAUTICS,
LANGLEY FIELD, VA., *October 10, 1935.*

TABLE I.—BLADE CHARACTERISTICS

Blade designation	Radius R	Span b_r	Chord c	Angle of zero lift α_{L_0}	Mass constant [1] $\gamma=\frac{c\rho a R^4}{I_1}$	Torsional rigidity [2] (deg. twist per in. length per in.-lb.)
	Feet	*Feet*	*Foot*	°		
A (N. A. C. A. 0012)----	5.00	4.375	0.523	0	5.31	0.00119
B (N. A. C. A. 0012)----	5.00	3.50	.523	0	5.28	.00088
C (N. A. C. A. 0012)----	5.00	2.75	.523	0	4.93	.00074
D (N. A. C. A. 0012)----	5.00	2.00	.523	0	4.62	.00057
A (N. A. C. A. 0018)----	5.00	4.375	.523	0	4.32	.00047
A (N. A. C. A. 4412)----	5.00	4.375	.523	−3.9	5.00	.00121
A (N. A. C. A. 4418)----	5.00	4.375	.523	−3.7	3.65	.00041

[1] Calculated for $\rho=0.002378$ slug/cu. ft.
[2] For torsional moment constant along blade.

REFERENCES

1. Weick, Fred E., and Wood, Donald H.: The Twenty-Foot Propeller Research Tunnel of the National Advisory Committee for Aeronautics. T. R. No. 300, N. A. C. A., 1928.
2. Jacobs, Eastman, N., Ward, Kenneth E., and Pinkerton, Robert M.: The Characteristics of 78 Related Airfoil Sections from Tests in the Variable-Density Wind Tunnel. T. R. No. 460, N. A. C. A., 1933.
3. Wheatley, John B.: An Aerodynamic Analysis of the Autogiro Rotor with a Comparison between Calculated and Experimental Results. T. R. No. 487, N. A. C. A., 1934.
4. Whittaker, E. T., and Robinson, G.: The Calculus of Observations. Blackie and Son, Ltd. (London), 1924.

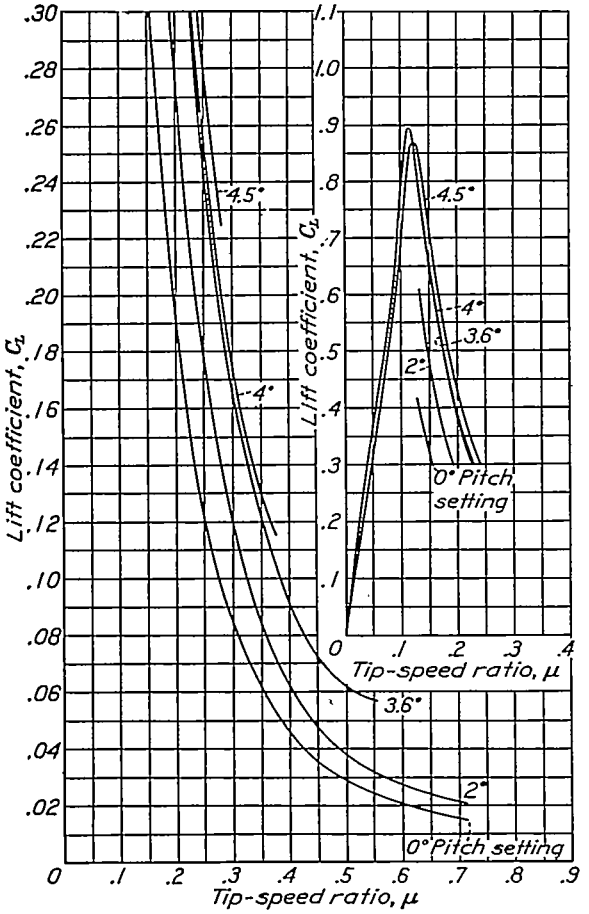

FIGURE 3.—Lift coefficient C_L of 10-foot autogiro rotor. A (N. A. C. A. 0012).

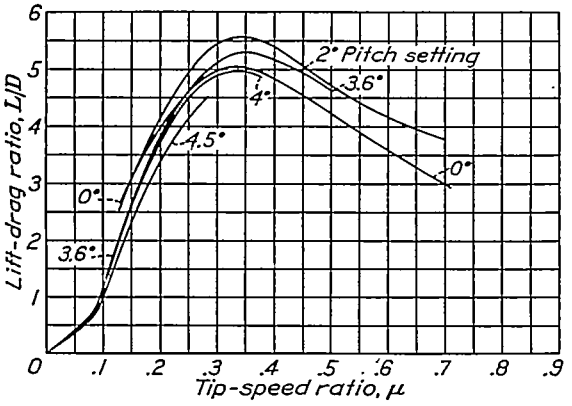

FIGURE 4.—Lift-drag ratio L/D of 10-foot autogiro rotor. A (N. A. C. A. 0012).

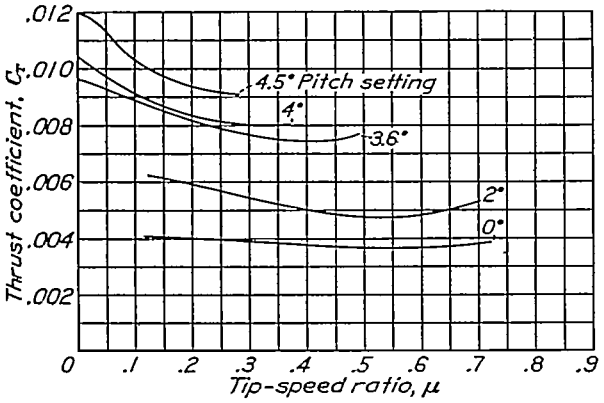

FIGURE 5.—Thrust coefficient C_T of 10-foot autogiro rotor. A (N. A. C. A. 0012).

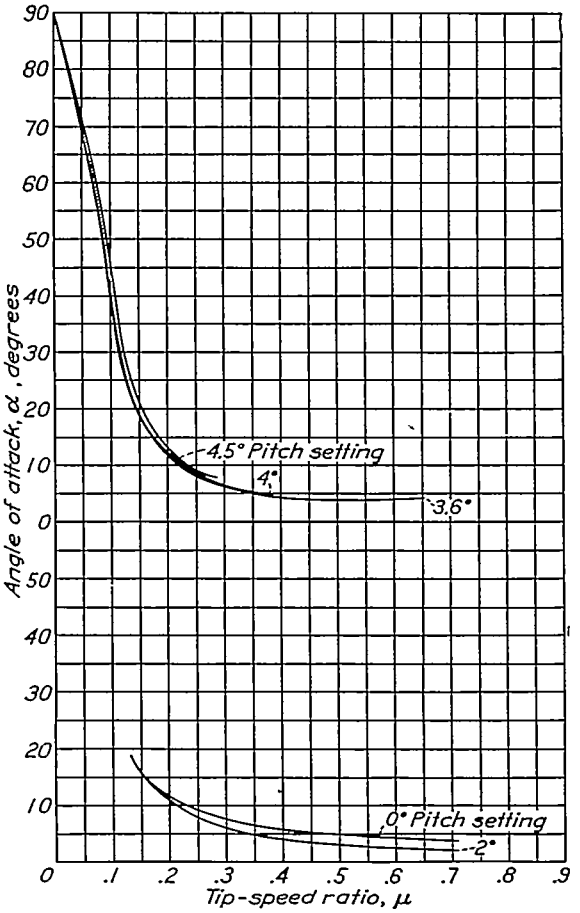

FIGURE 6.—Angle of attack α of 10-foot autogiro rotor. A (N. A. C. A. 0012).

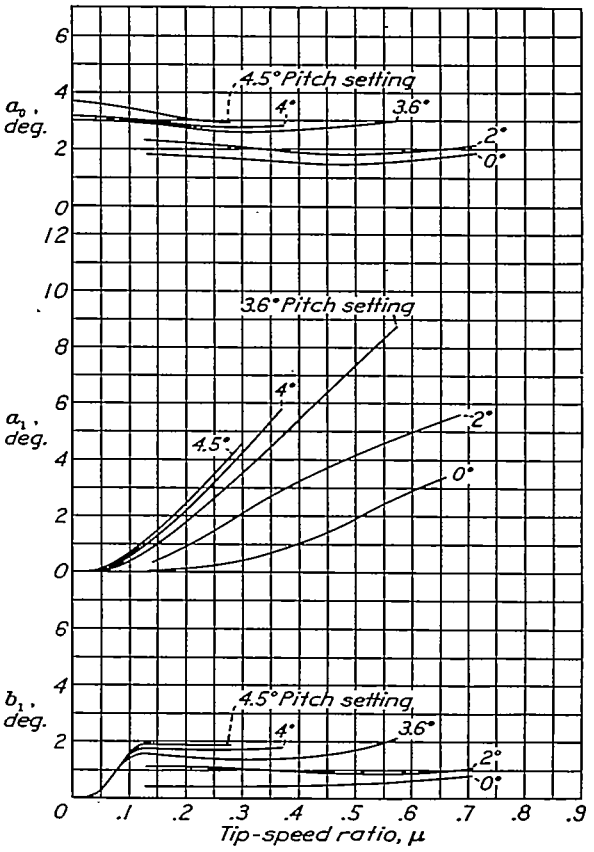

FIGURE 7.—Blade-motion coefficients a_0, a_1, and b_1 of 10-foot autogiro rotor. A (N. A. C. A. 0012.).

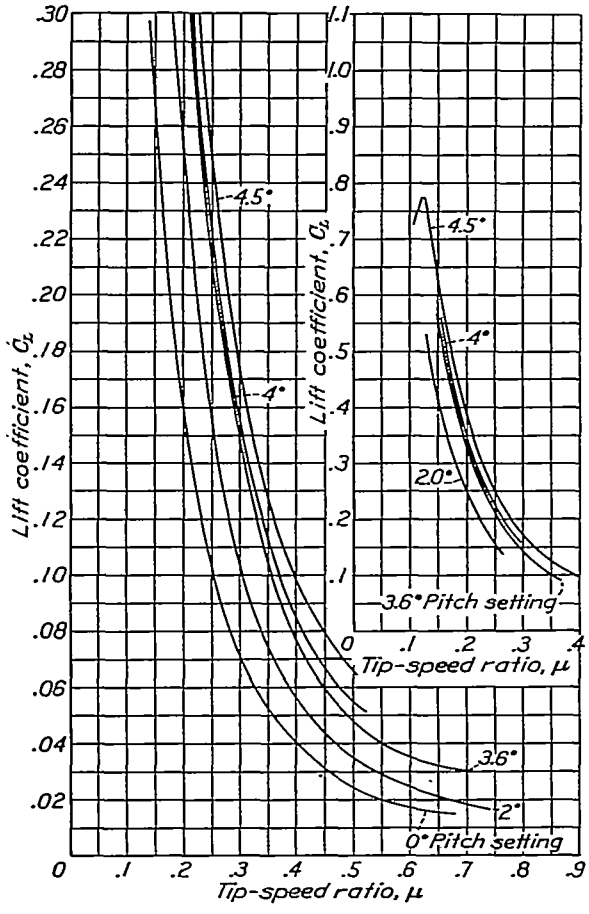

FIGURE 8.—Lift coefficient C_L of 10-foot autogiro rotor. B (N. A. C. A. 0012).

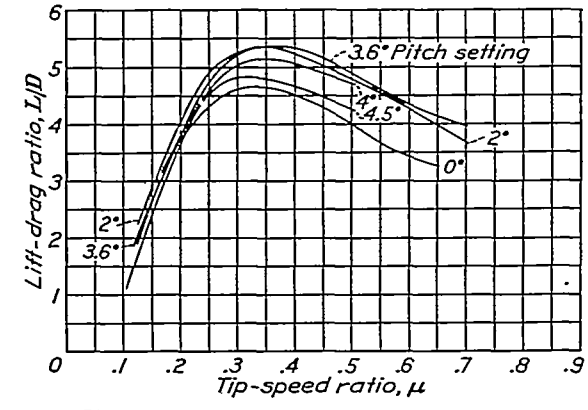

FIGURE 9.—Lift-drag ratio L/D of 10-foot autogiro rotor. B (N. A. C. A. 0012).

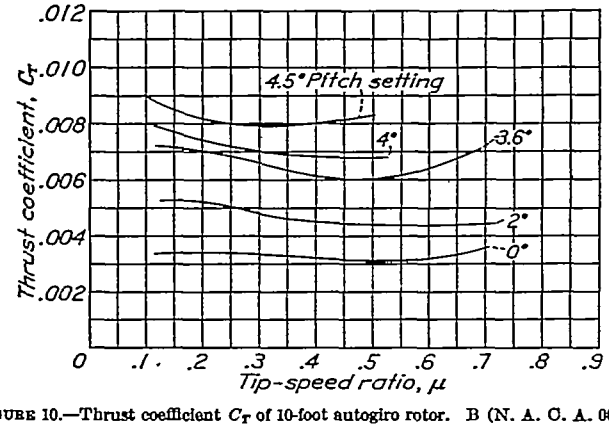

FIGURE 10.—Thrust coefficient C_T of 10-foot autogiro rotor. B (N. A. C. A. 0012).

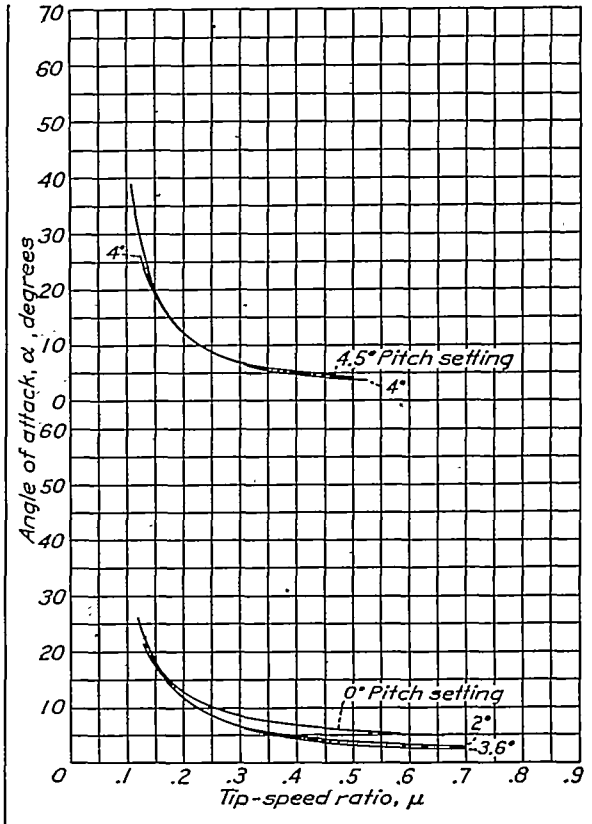

FIGURE 11.—Angle of attack α of 10-foot autogiro rotor. B (N. A. C. A. 0012).

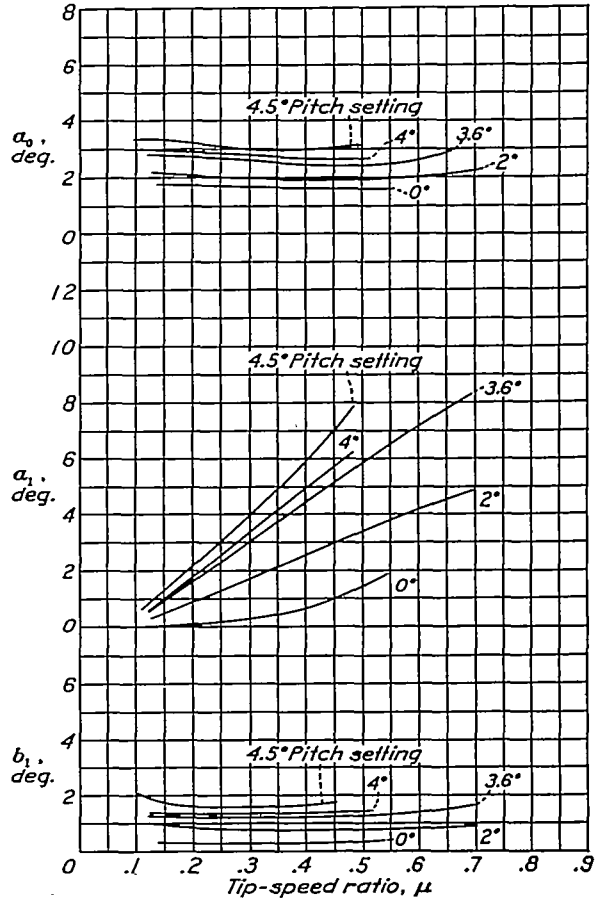

FIGURE 12.—Blade-motion coefficients a_0, a_1, and b_1 of 10-foot autogiro rotor. B (N. A. C. A. 0012).

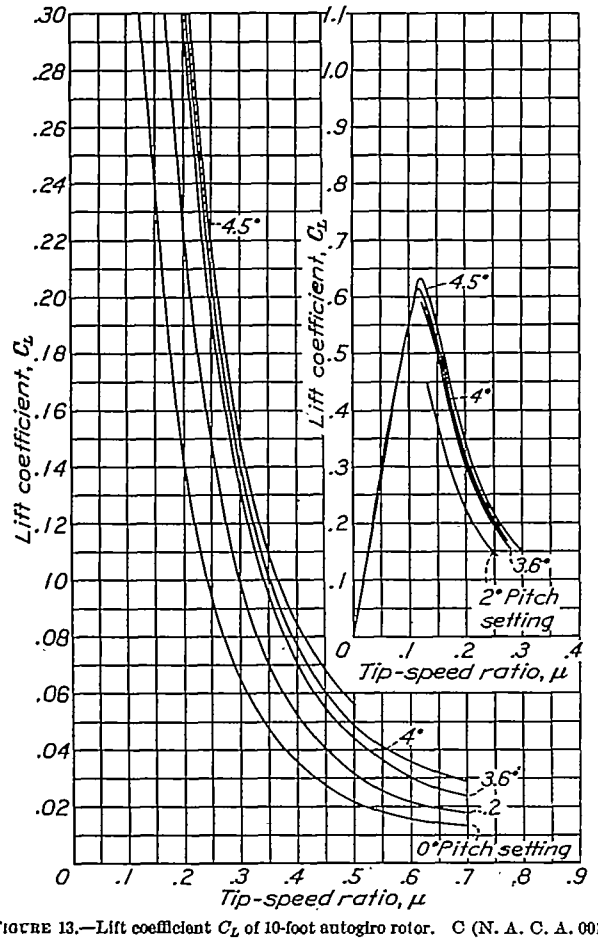

FIGURE 13.—Lift coefficient C_L of 10-foot autogiro rotor. C (N. A. C. A. 0012).

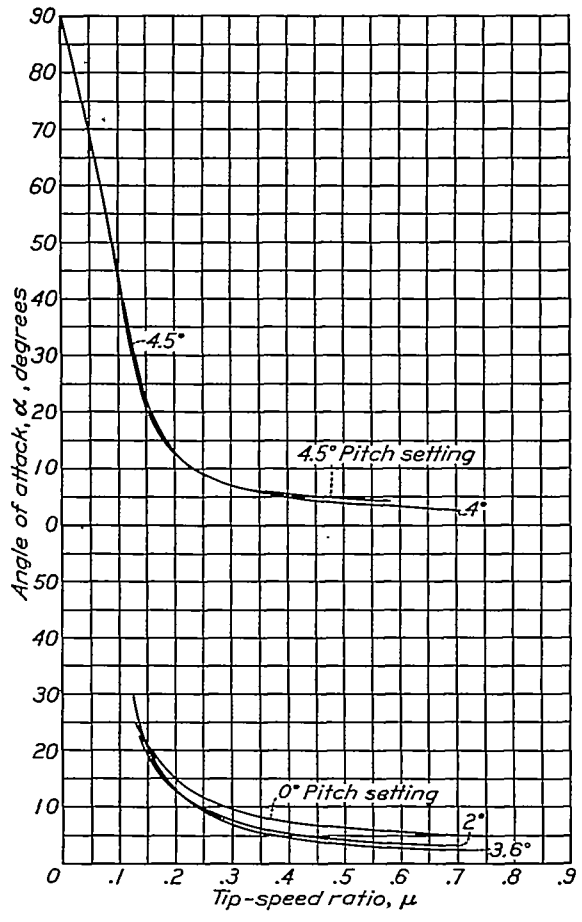

FIGURE 16.—Angle of attack α of 10-foot autogiro rotor. C (N. A. C. A. 0012).

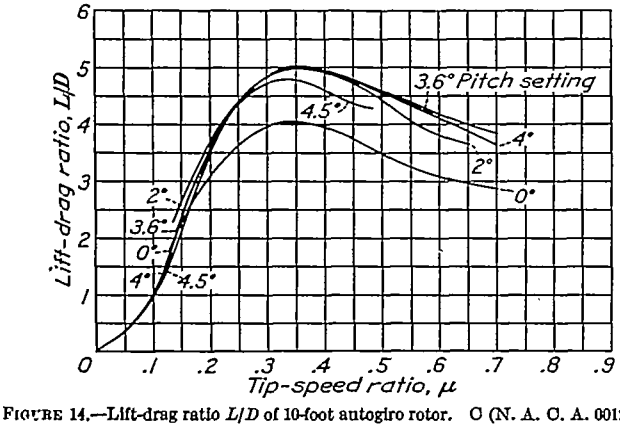

FIGURE 14.—Lift-drag ratio L/D of 10-foot autogiro rotor. C (N. A. C. A. 0012).

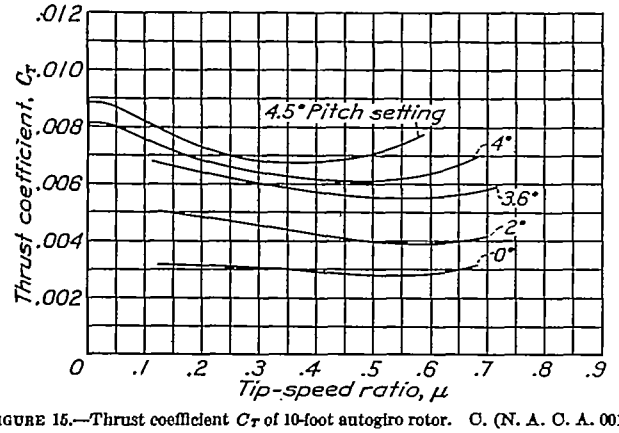

FIGURE 15.—Thrust coefficient C_T of 10-foot autogiro rotor. C. (N. A. C. A. 0012).

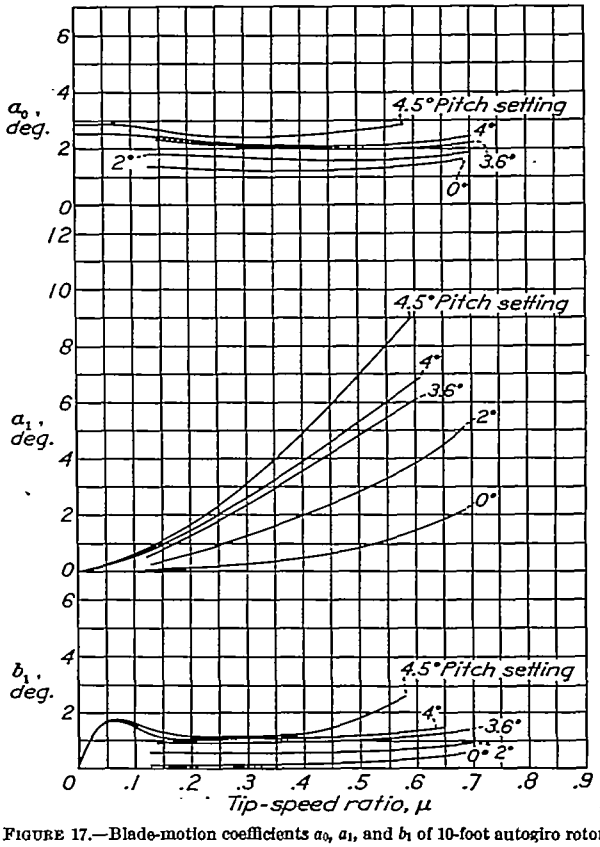

FIGURE 17.—Blade-motion coefficients a_0, a_1, and b_1 of 10-foot autogiro rotor. C. (N. A. C. A. 0012).

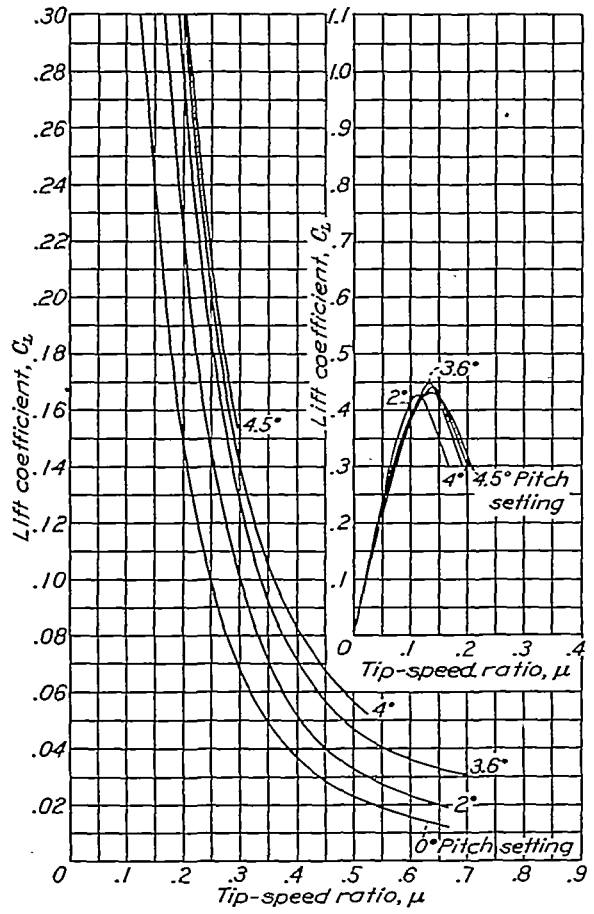

FIGURE 18.—Lift coefficient C_L of 10-foot autogiro rotor. D (N. A. C. A. 0012).

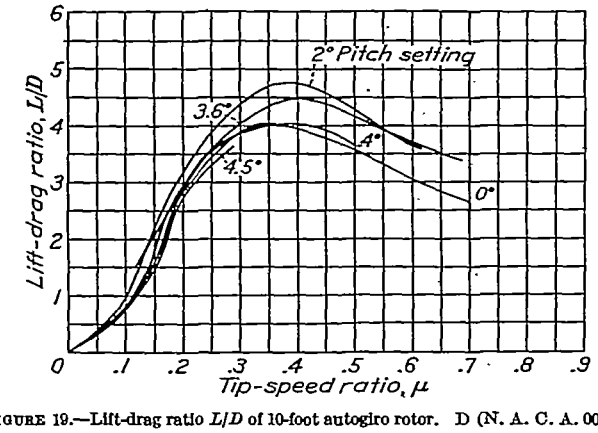

FIGURE 19.—Lift-drag ratio L/D of 10-foot autogiro rotor. D (N. A. C. A. 0012).

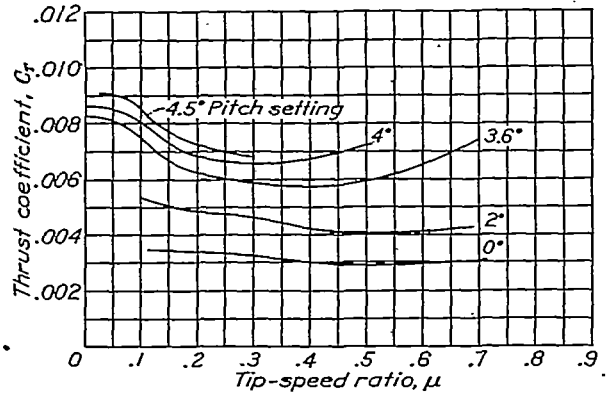

FIGURE 20.—Thrust coefficient C_T of 10-foot autogiro rotor. D (N. A. C. A. 0012).

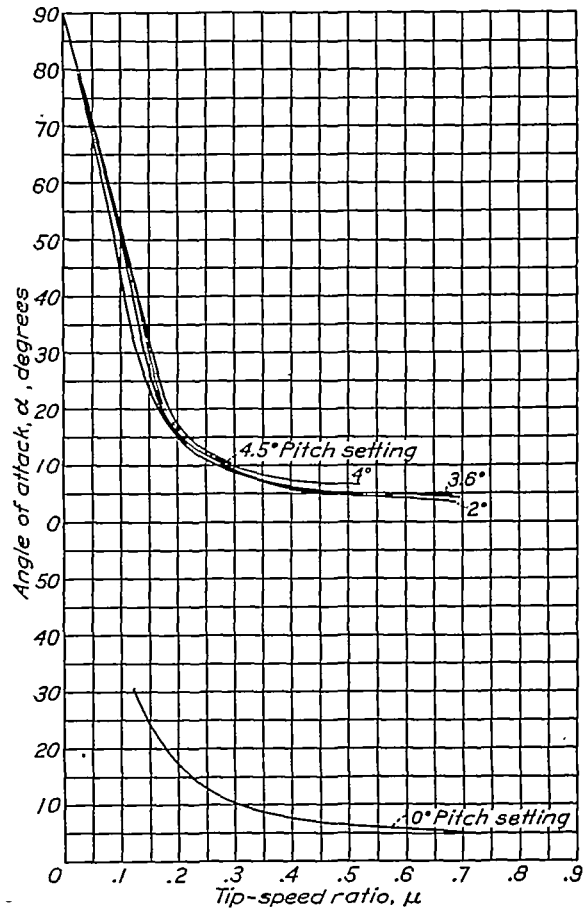

FIGURE 21.—Angle of attack α of 10-foot autogiro rotor. D (N. A. C. A. 0012).

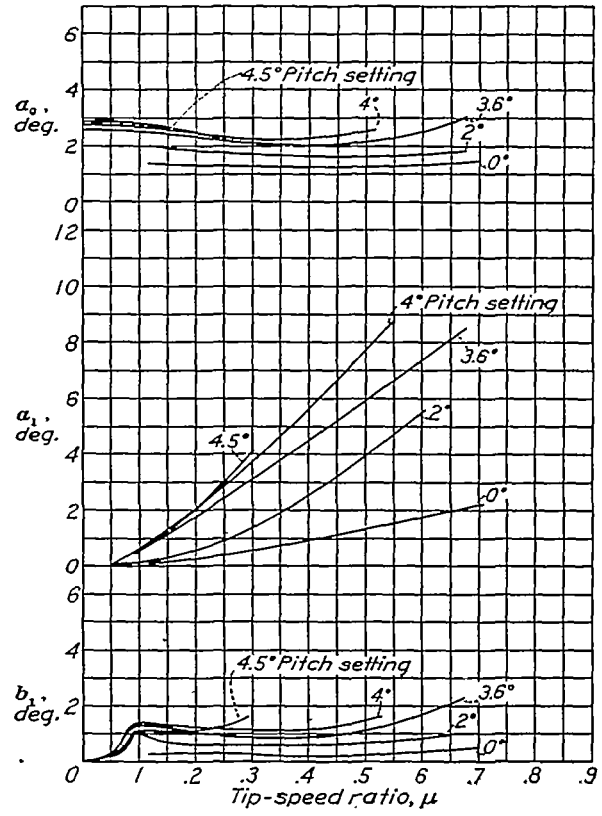

FIGURE 22.—Blade-motion coefficients a_0, a_1, and b_1 of 10-foot autogiro rotor. D (N. C. A. A. 0012).

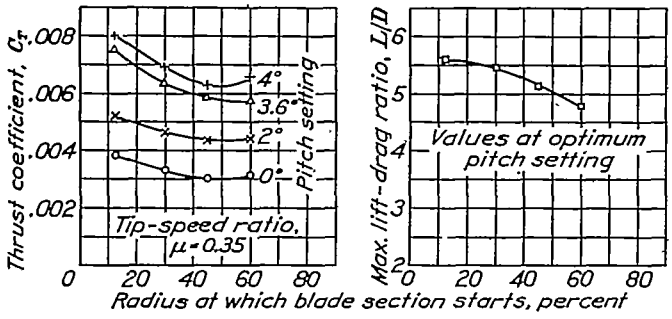

FIGURE 23.—Influence of blade span on maximum lift-drag ratio and thrust coefficient (at $\mu=0.35$) of 10-foot autogiro rotor.

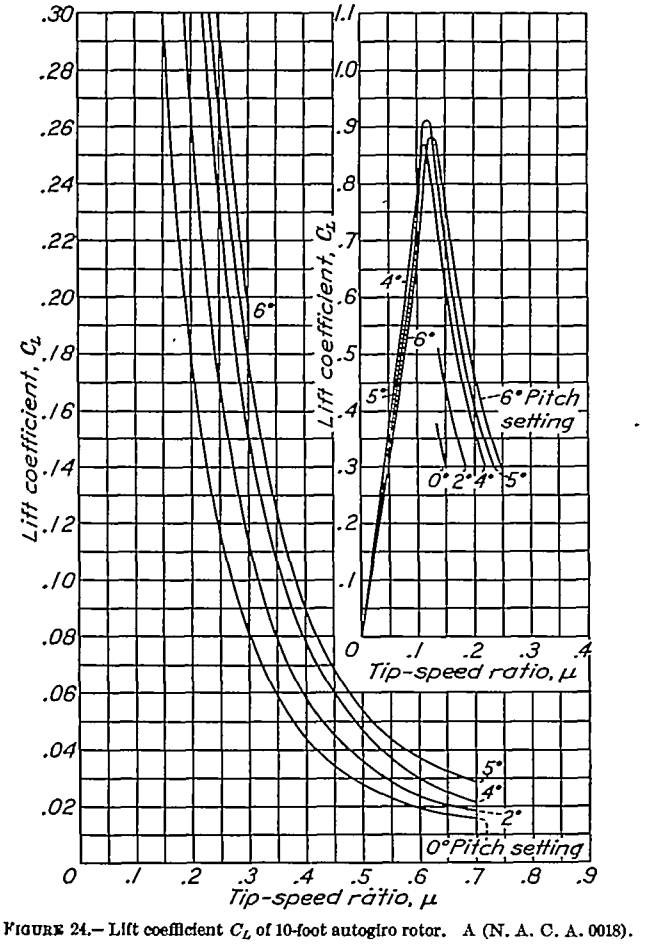

FIGURE 24.—Lift coefficient C_L of 10-foot autogiro rotor. A (N. A. C. A. 0018).

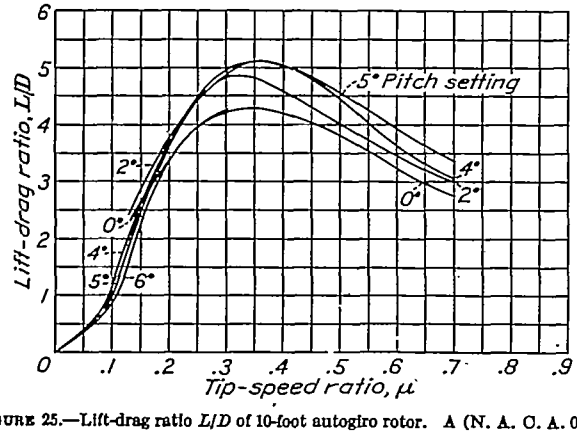

FIGURE 25.—Lift-drag ratio L/D of 10-foot autogiro rotor. A (N. A. C. A. 0018).

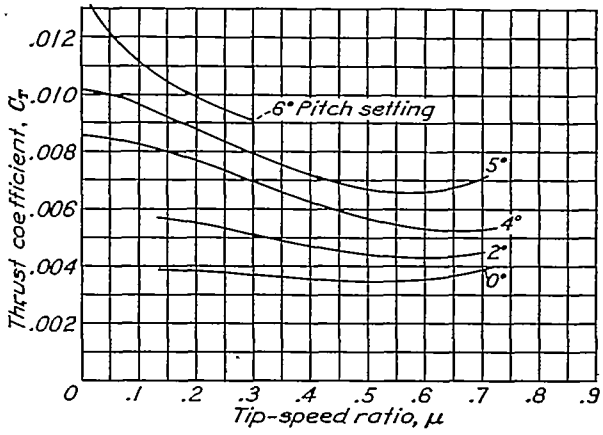

FIGURE 26.—Thrust coefficient C_T of 10-foot autogiro rotor. A (N. A. C. A. 0018)

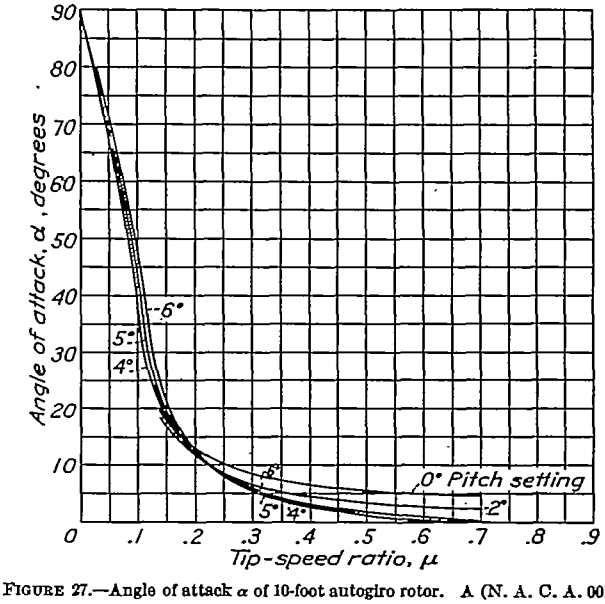

FIGURE 27.—Angle of attack α of 10-foot autogiro rotor. A (N. A. C. A. 0018).

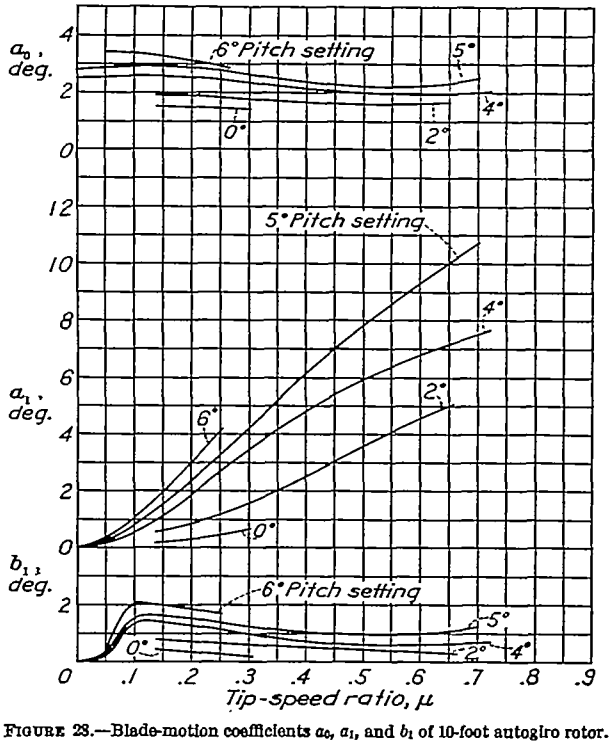

FIGURE 28.—Blade-motion coefficients a_0, a_1, and b_1 of 10-foot autogiro rotor. A (N. A. C. A. 0018).

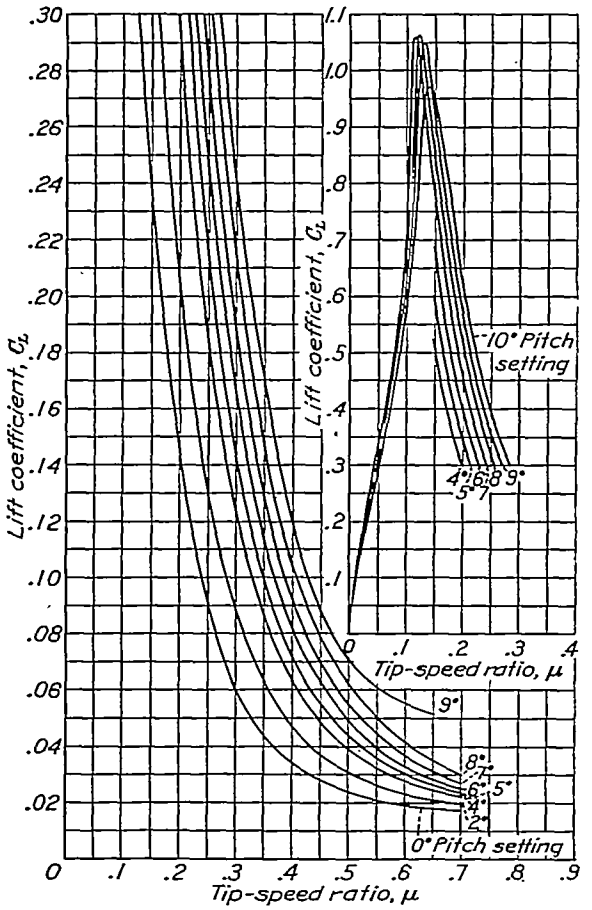

FIGURE 29.—Lift coefficient C_L of 10-foot autogiro rotor. A (N. A. C. A. 4412).

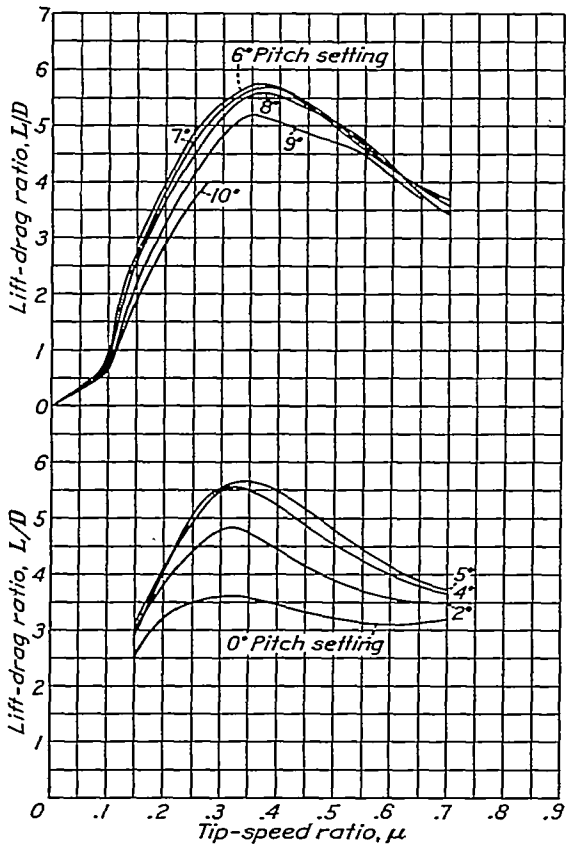

FIGURE 30.—Lift-drag ratio L/D of 10-foot autogiro rotor. A (N. A. C. A. 4412).

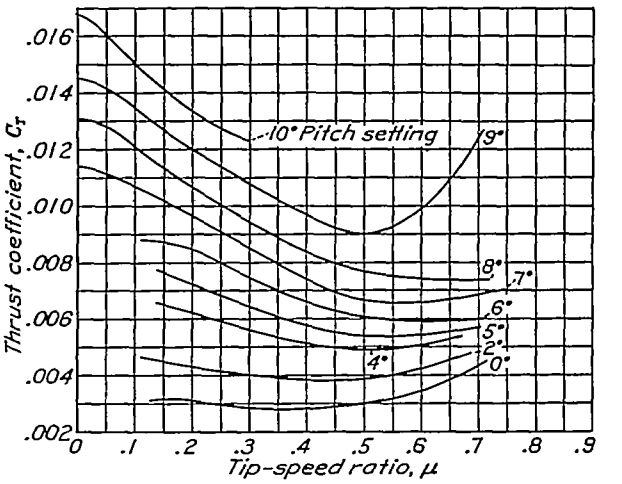

FIGURE 31.—Thrust coefficient C_T of 10-foot autogiro rotor. A (N. A. C. A. 4412).

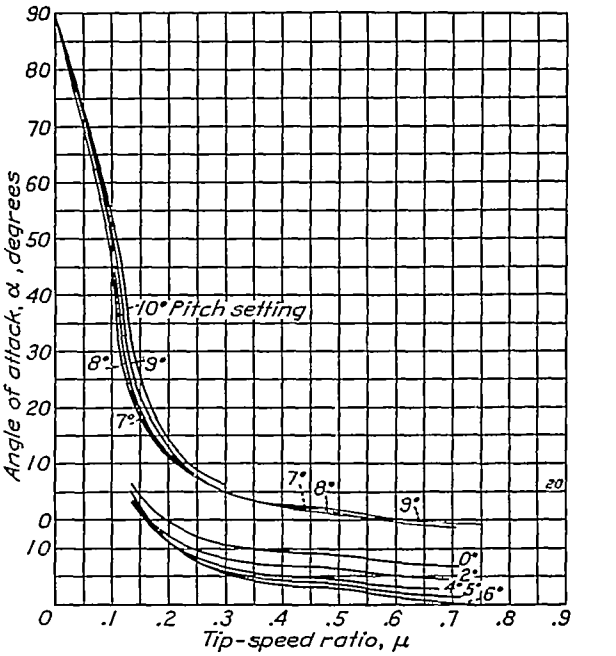

FIGURE 32.—Angle of attack α of 10-foot autogiro rotor. A (N. A. C. A. 4412).

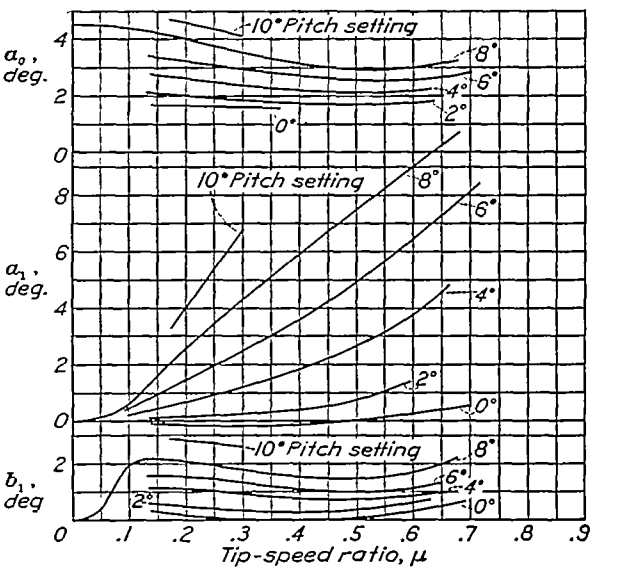

FIGURE 33.—Blade-motion coefficients a_0, a_1, and b_1 of 10-foot autogiro rotor A (N. A. C. A. 4412).

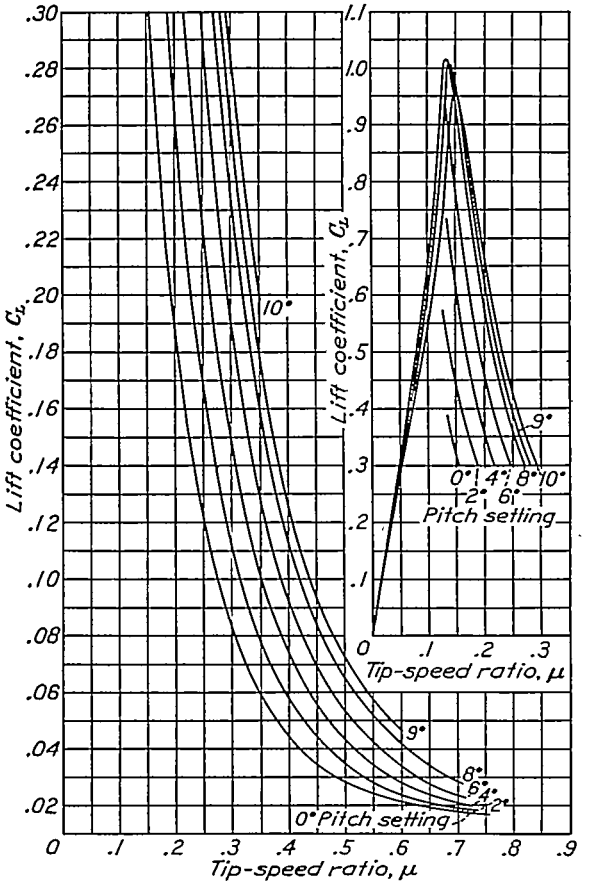

FIGURE 34.—Lift coefficient C_L for 10-foot autogiro rotor. A (N. A. C. A. 4418).

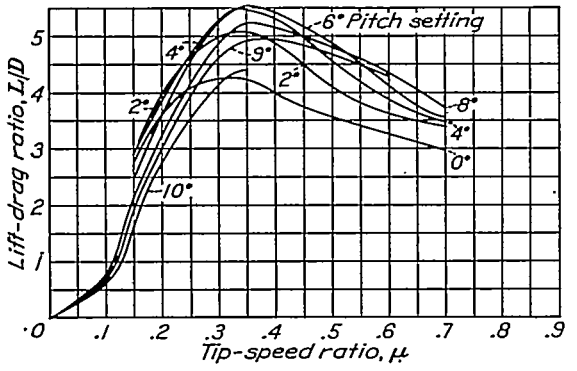

FIGURE 35.—Lift-drag ratio L/D of 10-foot autogiro rotor. A (N. A. C. A. 4418).

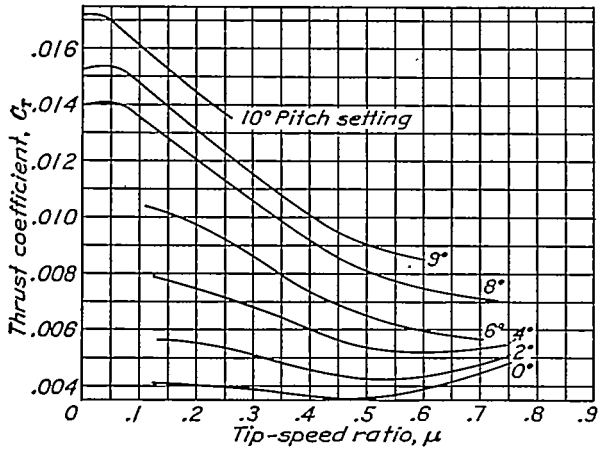

FIGURE 36.—Thrust coefficient C_T of 10-foot autogiro rotor. A (N. A. C. A. 4418).

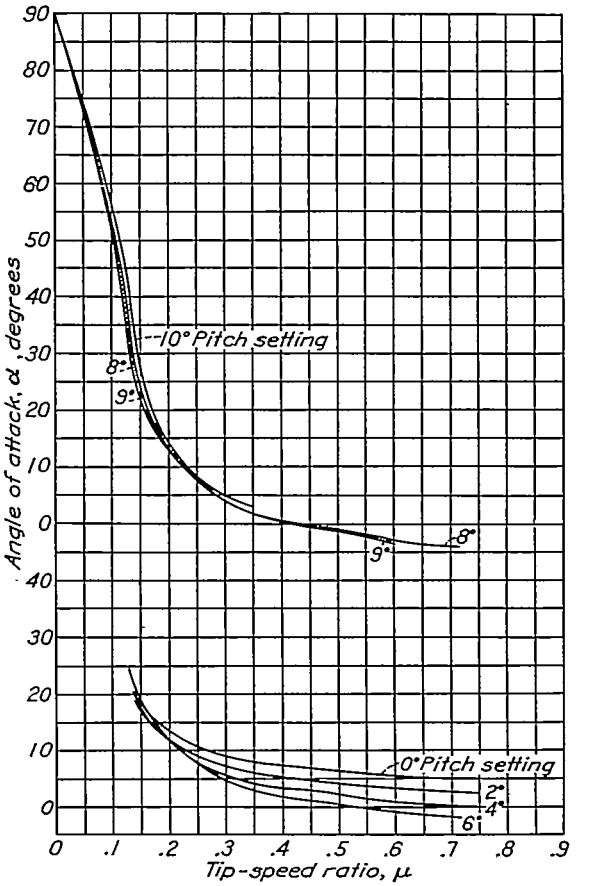

FIGURE 37.—Angle of attack α of 10-foot autogiro rotor. A (N. A. C. A. 4418)

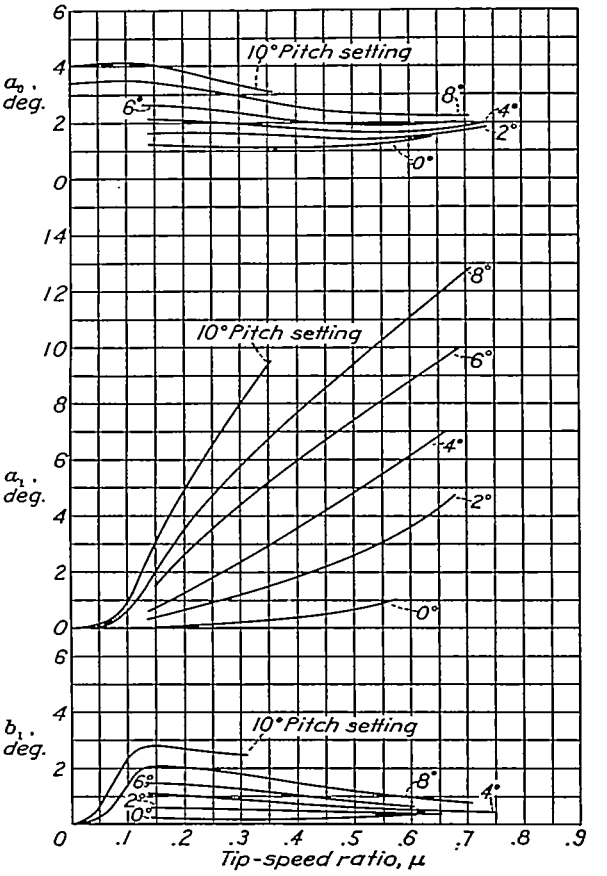

FIGURE 38.—Blade-motion coefficients a_0, a_1, and b_1 of 10-foot autogiro rotor. A (N. A. C. A. 4418).

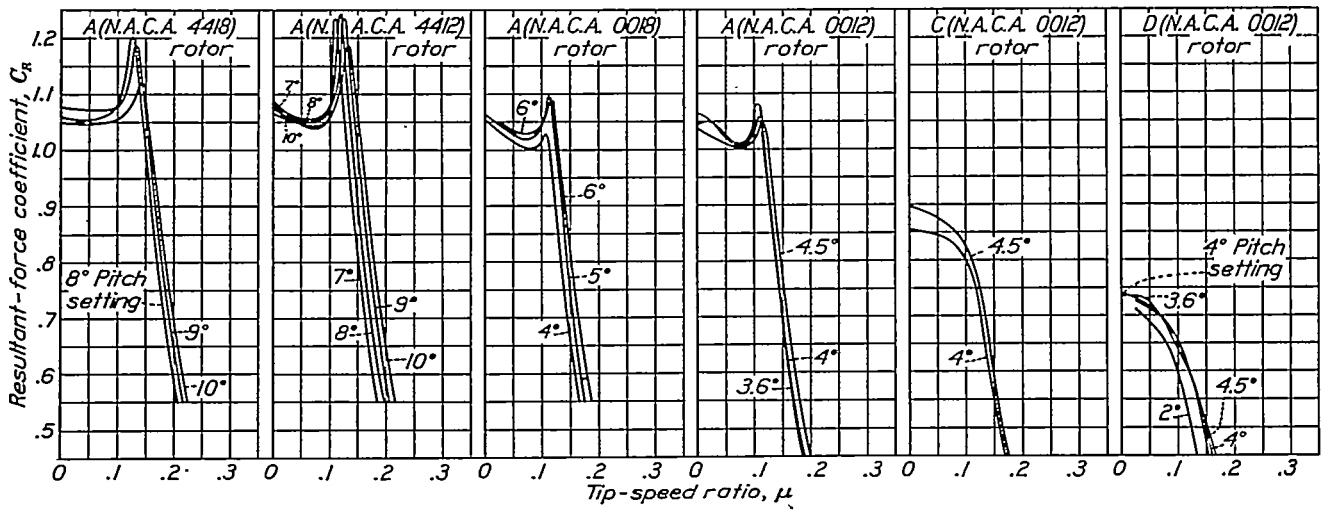

FIGURE 39.—Resultant-force coefficient C_R of 10-foot autogiro rotors.

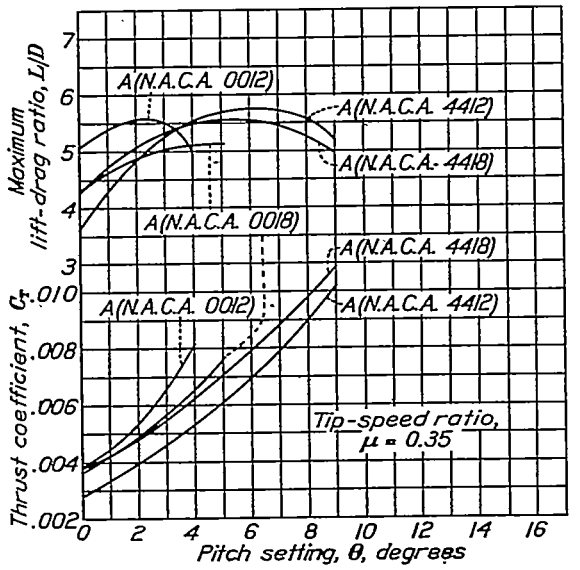

FIGURE 40.—Influence of pitch setting on maximum lift-drag ratio and thrust coefficient of 10-foot autogiro rotors.

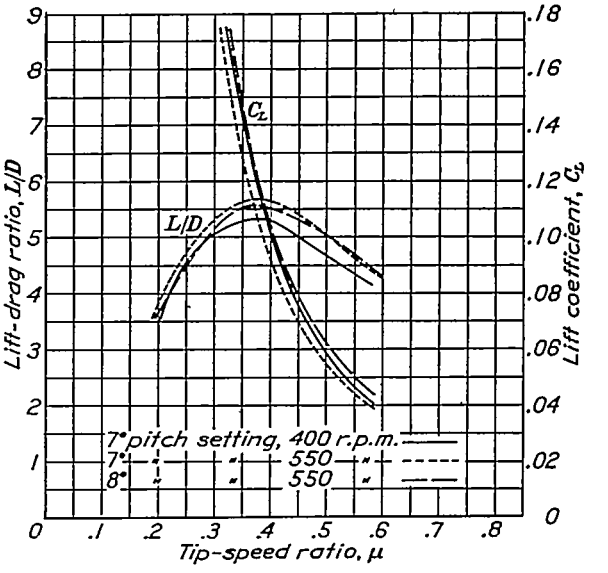

FIGURE 41.—Influence of rotor speed on lift coefficient and lift-drag ratio of 10 foot autogiro rotor. A (N. A. C. A. 4412).

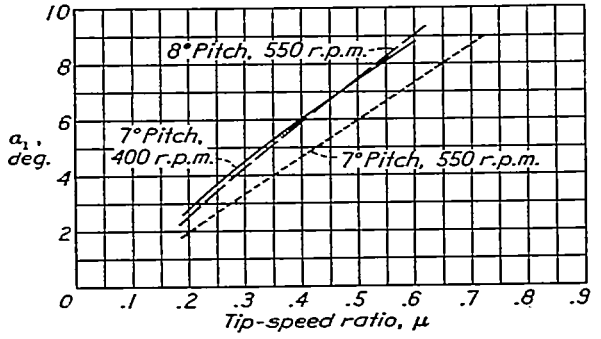

FIGURE 42.—Influence of rotor speed on flapping coefficient a_1 of 10-foot autogiro rotor. A (N. A. C. A. 4412).